ARMY RESEARCH LABORATORY

Thermo-Responsive Films Based Upon Diels-Alder Chemistry and Block Copolymer Phase Separation

by Philip J. Costanzo, Frederick L. Beyer, and J. Derek Demaree

ARL-TR-4127 June 2007

NOTICES

Disclaimers

The findings in this report are not to be construed as an official Department of the Army position unless so designated by other authorized documents.

Citation of manufacturer's or trade names does not constitute an official endorsement or approval of the use thereof.

Destroy this report when it is no longer needed. Do not return it to the originator.

Army Research Laboratory
Aberdeen Proving Ground, MD 21005-5069

ARL-TR-4127 **June 2007**

Thermo-Responsive Films Based Upon Diels-Alder Chemistry and Block Copolymer Phase Separation

Philip J. Costanzo, Frederick L. Beyer, and J. Derek Demaree
Weapons and Materials Research Directorate, ARL

REPORT DOCUMENTATION PAGE

Form Approved
OMB No. 0704-0188

1. REPORT DATE *(DD-MM-YYYY)*	2. REPORT TYPE	3. DATES COVERED (From - To)
June 2007	Interim	August 2005–January 2006

4. TITLE AND SUBTITLE
Thermo-Responsive Films Based Upon Diels-Alder Chemistry and Block Copolymer Phase Separation

5a. CONTRACT NUMBER

5b. GRANT NUMBER

5c. PROGRAM ELEMENT NUMBER

6. AUTHOR(S)
Philip J. Costanzo, Frederick L. Beyer, and J. Derek Demaree

5d. PROJECT NUMBER
AH42

5e. TASK NUMBER

5f. WORK UNIT NUMBER

7. PERFORMING ORGANIZATION NAME(S) AND ADDRESS(ES)
U.S. Army Research Laboratory
ATTN: AMSRD-ARL-WM-MA
Aberdeen Proving Ground, MD 21005-5069

8. PERFORMING ORGANIZATION REPORT NUMBER
ARL-TR-4127

9. SPONSORING/MONITORING AGENCY NAME(S) AND ADDRESS(ES)

10. SPONSOR/MONITOR'S ACRONYM(S)

11. SPONSOR/MONITOR'S REPORT NUMBER(S)

12. DISTRIBUTION/AVAILABILITY STATEMENT
Approved for public release; distribution is unlimited.

13. SUPPLEMENTARY NOTES

14. ABSTRACT
The surface properties of poly(ethylene glycol) (PEG) films have been modified using gold particles functionalized with block copolymer-based ligands of poly(styrene) (PS) and PEG. The ligands were synthesized using Diels-Alder chemistry to join the PS and PEG blocks into linear diblock copolymers, which were attached to gold particles with a thiol terminal functionality on the PS block. The block copolymer ligands compatibilized the Au particles by creating a PEG shell around the Au and PS core. The Diels-Alder linkage, however, is temperature sensitive, and by annealing the films at 90 °C, the PEG blocks of the ligand were separated from the PS-functionalized Au core. The Au particles were thus rendered immiscible in the PEG matrices and migrated to the film surfaces.

15. SUBJECT TERMS
miscibility, gold, nanoparticle, immiscibility, ligand

16. SECURITY CLASSIFICATION OF:			17. LIMITATION OF ABSTRACT	18. NUMBER OF PAGES	19a. NAME OF RESPONSIBLE PERSON
a. REPORT	b. ABSTRACT	c. THIS PAGE			Frederick L. Beyer
UNCLASSIFIED	UNCLASSIFIED	UNCLASSIFIED	UL	26	19b. TELEPHONE NUMBER (*Include area code*) 410-306-0893

Standard Form 298 (Rev. 8/98)
Prescribed by ANSI Std. Z39.18

Contents

List of Figures

Acknowledgments

The authors thank Professor Timothy Patten for donating α-mercapto-ω-methoxy PEG and α-mercapto-ω-methoxy PS-b-PEG polymer samples. Mr. Kris Stokes (Massachusetts Institute of Technology) and Dr. Josh Orlicki, U.S. Army Research Laboratory (ARL), are acknowledged for their helpful discussions. Funding was provided by ARL. Philip J. Costanzo was supported by a post-doctoral fellowship administered by the Oak Ridge Institute for Science Education.

INTENTIONALLY LEFT BLANK.

1. Introduction

The development of stimuli responsive films has been explored and studied for many applications, including tissue engineering (*1*, *2*), permeable membranes (*3*), and packaging materials (*4*). These materials undergo a dramatic change in their physical properties due to a global radiation stimulus, such as temperature, pH, or light. Such responsive materials impart utility to the user and create a platform for the development of more complex devices.

Block copolymer phase separation has been employed as an approach to prepare functionalized polymer surfaces. A wide range of techniques have been utilized to study and prepare phase segregated polymer surfaces (*5–17*). Of particular relevance is the work of the Koberstein group, which has not only prepared a variety of systems focusing on the effects of variations in polymer architecture and composition, but also provided extensive modeling of their systems to explain the observed phenomena (*18*, *19*). They have demonstrated the mobilization, also referred to as "blooming," of chain-end fluorinated poly(styrene) (PS) to the surface of a poly(dimethylsiloxane) (PDMS) spin coated film. It was found that the key driving force for blooming is the reduction of surface energy. One limiting characteristic of this approach is that the blooming of molecules immediately occurs. For some applications, it may be more important to control the timing with which the surface of a material is modified.

Diels-Alder (DA) chemistry offers the needed characteristics to control the blooming of polymers to the surface (*20*, *21*). Recently, many research groups have exploited the combination of DA chemistry and block copolymers to prepare organic-inorganic polymer hybrids (*22*), thermoplastic elastomers (*23*, *24*), polyurethanes, and foams (*4*). The goal of this study is the fabrication of a film that is sensitive to a global, external stimulus. We propose using DA chemistry to create appropriate block copolymer ligands which would be used to disperse nanoparticles in a polymer matrix. Due to the temperature dependent reversibility of the DA linkage between the two blocks in the ligand, application of appropriate thermal conditions should sever the outer block of the ligand, resulting in a particle that is modified with a ligand that renders the particle immiscible in the polymer matrix. The combination of immiscibility and mobility at elevated temperatures should allow the functional particles to bloom to the surface of the polymer film, completing the material response to the external stimulus.

2. Experimental

2.1 Materials

All materials were purchased from commercially available sources. Styrene was dried with CaH_2 and distilled under vacuum. All other materials were used without further purification. α-Mercapto-ω-methoxy PEG and α-mercapto-ω-methoxy PS-b-PEG were donated from the University of California at Davis (*25*).

2.2 Instrumentation and Analysis

2.2.1 Nuclear Magnetic Resonance

^{1}H and ^{13}C nuclear magnetic resonance (NMR) were conducted on a Bruker-Biospin 600-MHz Ultrashield Avance spectrometer with a standard bore broadband probe (5-mm-OD tubes, 32 scans, 5-s d1). Spectra were recorded in $CDCl_3$, and all resonances were reported as ppm reference to the residual solvent peak (δ 7.26 ppm). Number average molecular weights (M_n) and polydispersities (PDI) were determined using a gel-permeation chromatography (GPC) in tetrahydrofuran (THF) at 25 ºC and at a flow rate of 1.00 mL/min. Three Polymer Standards Service columns (10^3 Å, 10^4 Å, and 10^5 Å) were connected in a series to a high-performance liquid chromatography (HPLC) isocratic pump, autosampler, ultraviolet detector, and Wyatt DAWN MALLS and OPTLAB refractive index detector.

2.2.2 Contact Angle Measurements

Contact angle measurements were recorded using a goniometer equipped with a charge-coupled-device camera and an image capture program employing LabView software. Contact angles were measured using HPLC-grade water by defining a circle about the drop and recording the tangent angle formed at the substrate surface.

2.2.3 Transmission Electron Microscopy

Transmission electron microscopy (TEM) was completed using a JEOL 200 CX instrument operated at 120-kV accelerating voltage. Samples of ligand-modified particles for TEM were prepared by drop-casting solutions of the particles in THF onto Formvar-coated TEM grids. Image analysis for particle size and distribution was performed using ImageJ, available free of charge from the National Institute of Health (NIH) website (*26*). Threshold was set to include at least 2000 counts using 100 bins with a minimum pixel size of 5.

2.2.4 Rutherford Backscattering Spectroscopy

Rutherford backscattering spectroscopy (RBS) experiments were performed using 1.2-MeV He^+ ion beams from an NEC 5SDH-2 tandem positive ion accelerator. The backscattering angle was 170°, and the solid angle of the surface barrier detector was approximately 4 millisteradians. When it was necessary to enhance the depth resolution, the samples were titled with respect to the beam in an "IBM" configuration: the surface normal coplanar with the incoming ion beam and the direction of the scattered ions. All spectra were fit and interpreted using the program RUMP (*27*).

2.2.5 Small-Angle X-ray Scattering

Small-angle x-ray scattering (SAXS) data were collected using the U.S. Army Research Laboratory SAXS instrument, which consists of a Rigaku Ultrax18 rotating Cu anode x-ray generator (operated at 40 kV, 115 mA), a customized 1.5-m three pinhole camera, and a

molecular metrology two-dimensional (2-D) multiwire area detector. Cu-Kα radiation was selected using a Ni filter. The sample-to-detector distance was approximately 1.1 m. Liquid samples were run using a molecular metrology liquid sample cell in which the sample is contained between mica windows and has a sample thickness of 1 mm. Two-dimensional data were corrected for background and detector noise prior to azimuthally averaging. One-dimensional data are presented as intensity, $I(q)$, as a function of the magnitude of the scattering vector, $q = 4\pi \cdot \sin(\theta)/\lambda$, where 2θ is the scattering angle and λ is the x-ray wavelength (1.542 Å). Absolute scaling was achieved using type-2 glassy carbon as a secondary standard (*28*). All data corrections and analysis were performed using Wavemetrics Igor Pro 5.04B and procedure packages compiled by Dr. Jan Ilavsky of the Argonne National Laboratory. To analyze particle size, SAXS data were collected from oleylamine-stabilized Au particles in toluene (*29*). The ligand was used to promote solubility of the particles and prevent particle aggregation. Oleylamine was chosen specifically for its low molecular weight, simplifying the modeling of the particle form factor. Successive dilutions were examined until no evidence of interparticle scattering was observed, which was found empirically to occur at a concentration of 0.148 mg/mL of the stabilized Au particles. To analyze particle size, a log-normal size distribution of particle volume was input into the form factor for a spherical particle, generating model scattering data.

2.3 Synthesis of Materials

2.3.1 Synthesis of Furyl-2-Bromopropionate (1)

Furyl alcohol (5.00 mL, 58.0 mmol), triethylamine (Et_3N) (10.5 mL, 75.4 mmol), and CH_2Cl_2 (150 mL) were added to a 250-mL round bottom flask and cooled to 0 ºC. Next, 2-bromoprionyl bromide (7.30 mL, 69.0 mmol) was added dropwise slowly. The reaction mixture was stirred at RT for 12 hr. H_2O (150 mL) was added, and the reaction was then extracted with CH_2Cl_2 (2 × 100 mL), which was collected and dried over anhydrous $MgSO_4$. Solvent was removed via rotary evaporation to yield 1 (12.1 g, 89 %) as a yellow liquid. ^{1}H NMR: δ (ppm) 7.42 (1 H, s), 6.42 (1 H, d), 6.38 (1 H, d), 5.13 (2 H, q), 4.37 (1H, q), 1.79 (1H, d); ^{13}C {^{1}H} NMR 169.9, 148.7, 143.5, 111.7, 110.7, 59.3, 39.6, 21.6.

2.3.2 Synthesis of Furyl S-Thiobenzoyl-2-Thiopropionate (2)

Compound 1 and a stir bar were loaded into a 100-mL schlenk flask which was vacuum/backfilled three times with N_2. THF (20 mL) was added and the reaction was stirred. In a 25-mL round bottom flask, a stir bar was loaded and then vacuum/backfilled three times with N_2. Phenyl magnesium chloride (12.8 mL, 25.7 mmol) and THF (10 mL) were then added. The 25-mL round bottom flask was cooled to –78 ºC, and while stirring CS_2 (1.50 mL, 25.7 mmol) was added. The reaction stirred for 15 min at –78 ºC and then for 1 hr at room temperature. The contents of the round bottom flask were then transferred to the 100-mL schlenk flask via cannula, and the reaction stirred for 5 hr at RT. The reaction mixture was partitioned after the addition of H_2O (75 mL). The aqueous layer was then extracted with EtOAc (2 × 50 mL), and

the organic layers were combined and dried over anhydrous $MgSO_4$. Solvent was removed via rotary evaporation to yield 2 (6.31 g, 96 %) as a red liquid. ^{1}H NMR: δ (ppm) 7.94 (1 H, d), 7.55 (2 H, t), 7.42 (1 H, s), 7.39 (2 H, t), 6.42 (1 H, d), 6.38 (1 H, d), 5.13 (2 H, s), 4.75 (1 H, q), 1.79 (3 H, d); ^{13}C {^{1}H} NMR 225.5, 170.9, 149.0, 144.5, 143.5, 132.8, 128.9, 127.0, 111.7, 110.7, 59.3, 48.7, 17.4.

2.3.3 Synthesis of α-methoxy-ω-maleimido poly(ethylene glycol) (Polymer 1)

Poly(ethylene glycol) (550 g/mol; PDI < 1.05) (5.00 g, 9.10 mmol), Et_3N (1.68 mL, 12.0 mmol), CH_2Cl_2 (80 mL), and a stir bar were placed into a 250-mL flat bottom flask and cooled to 0 ºC. Methanesulfonyl chloride (0.78 mL, 10.0 mmol) was added dropwise slowly. The flask was warmed to room temperature and stirred for 4 hr. Next, solid K_2CO_3 (2 g) and maleimide (1.16 g, 12.0 mmol) dissolved in THF (20 mL) were added. The reaction was then stirred at reflux for 12 hr. The reaction was cooled to room temperature and extracted with CH_2Cl_2 (3 × 100 mL), which was collected and dried over anhydrous $MgSO_4$. Solvent was removed via rotary evaporation to yield polymer 1 (5.45 g, 95 %) as a yellow oil. ^{1}H NMR: δ (ppm) 6.55 (1 H, s), 4.25 (2 H, t), 3.41-3.68 (38 H, m).

2.3.4 RAFT Polymerization of α-furyl-ω-S-thiobenzoyl poly(styrene) (Polymer 2)

Compound 2 (1.00 g, 3.24 mmol), azobisisobutyronitrile (AIBN) (780 mg, 4.80 mmol), styrene (18.4 mL, 160 mmol), THF (40 mL), and a stir bar were added to a 100-mL round bottom flask. The reaction mixture was purged with N_2 for 30 min and then heated at 70 ºC for 19 hr. The reaction was cooled to RT, and the polymer was isolated by precipitation into CH_3OH to isolate polymer 2 (11.0 g, 67%) as a pink powder. GPC: M_n - 4600 g/mol (PDI - 1.14).

2.3.5 Reduction of α-furyl-ω-S-thiobenzoyl poly(styrene) (Polymer 3)

Polymer 2 (10.6 g, 2.3 mmol) and a stir bar were loaded into a 250-mL flat bottom flask. THF (70 mL), EtOH (70 mL), and $NaBH_4$ (870 mg, 23 mmol) were added to the flask in that order. The reaction stirred for 20 hr at RT. Solvent was removed via rotary evaporation. THF (10 mL) was added, and subsequent precipitation into CH_3OH yielded polymer 3 (quantitative yield) as a white powder.

2.3.6 Diels-Alder Reaction Between Polymer 1 and 2 (1-DA-2 Copolymer)

Polymer 1 (1.3 g, 2.0 mmol), polymer 2 (0.75 g, 0.19 mmol), THF (7 mL), and a stir bar were loaded into a 15-mL round bottom flask. The reaction was stirred at 60 ºC for 5 days. The reaction was cooled to RT and upon precipitation into CH_3OH yielded 1-DA-2 copolymer (200 mg, 23%) as a white powder. To demonstrate reversibility, 1-DA-3 copolymer (100 mg, 0.022 mmol), toluene (4 mL), and a stir bar were loaded into a 10-mL round bottom flask. The reaction was stirred at 90 ºC for 12 hr. The reaction was cooled to RT and an analytic sample was isolated from precipitation into CH_3OH (see figure 1) for ^{1}H NMR spectra.

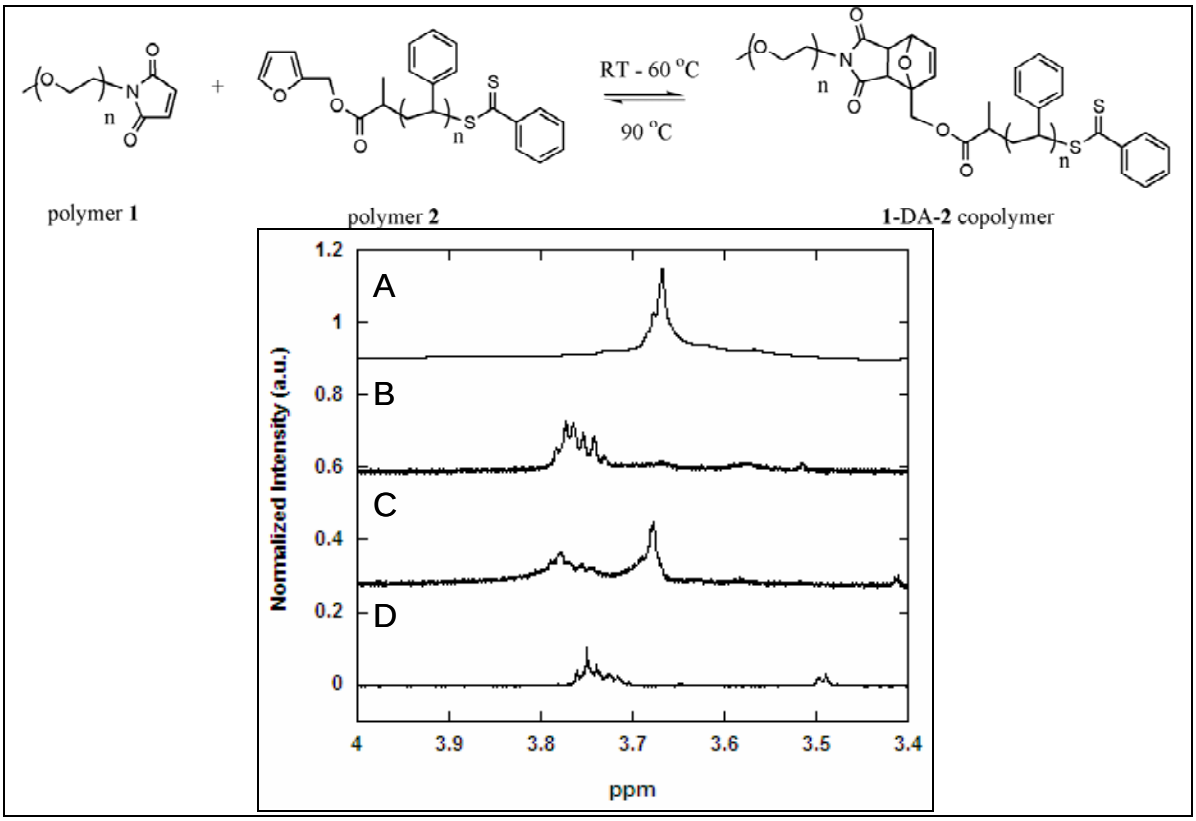

Figure 1. Top: Schematic of model compounds utilized to demonstrate reversible Diels-Alder chemistry. Bottom: 1H NMR of polymer 1, polymer 2, and 1-DA-2-copolymer. (a) 1H NMR of polymer 1; (b) 1H NMR of polymer 2; (c) 1H NMR of isolated polymer after heating polymer 1 and polymer 2 at 60 ºC for 5 days, resulting in 1-DA-2-copolymer; (d) 1H NMR of isolated polymer after heating 1-DA-2-copolymer at 90 ºC for 12 hr, resulting in polymer 2. (Note: A, B, and C are offset by 0.90, 0.59, and 0.27 a.u., respectively, for clarity.)

2.3.7 Preparation of Furyl Functionalized Au Nanoparticles (Polymer 3-Au)

Polymer 3 (4.6 g, 1.0 mmol), toluene (25 mL), and a stir bar were loaded into a 100-mL round bottom flask and stirred at reflux. Next, Au nanoparticles (81 mg, ~ 0.8 mmol of ligand) suspended in toluene (10 mL) were added, and the reaction proceeded to stir at reflux for 2 hr. The reaction was cooled to RT, and the particles were isolated by a series of centrifugation, decanting, and resuspension (5×) with THF/EtOH (3:2). Volatile materials were removed under vacuum to yield polymer 3-Au (1.3 g) as a magenta powder.

2.3.8 Functionalization of Au Nanoparticles With α-mercapto-ω-methoxy (PEG-p(St)-Au)

α-Mercapto-ω-methoxy PEG (500 mg, 0.1 mmol), toluene (8 mL), and a stir bar were loaded into a 25-mL round bottom flask and stirred at reflux. Next, Au nanoparticles (10 mg, ~ 0.01 mmol of ligand) suspended in toluene (2 mL) were added, and the reaction proceeded to stir at reflux for 2 hr. The reaction was cooled to RT, and the particles were isolated by a series of centrifugation, decanting, and resuspension (5×) with CH_3OH. Volatile materials were removed under vacuum to yield PEG-Au (64 mg) as a magenta powder.

2.3.9 Functionalization of Au Nanoparticles With α-mercapto-ω-methoxy poly(styrene)-b-PEG (PEG-p(St)-Au)

α-Mercapto-ω-methoxy poly(styrene)-b-PEG (1 g, 0.025 mmol), toluene (8 mL), and a stir bar were loaded into a 25-mL round bottom flask and stirred at reflux. Next, Au nanoparticles (10 mg, ~0.01 mmol of ligand) suspended in toluene (2 mL) were added, and the reaction proceeded to stir at reflux for 2 hr. The reaction was cooled to RT, and the particles were isolated by a series of centrifugation, decanting, and resuspension (5×) with THF/EtOH (3:2). Volatile materials were removed under vacuum to yield PEG-b-PS-Au (750 mg) as a magenta powder.

2.3.10 Diels-Alder Reaction Between Polymer 1 and Polymer 3-Au (1-DA-3 Au)

Polymer 1 (630 mg, 1.0 mmol), polymer 3-Au (1.3 g), THF (40 mL), and a stir bar were loaded into a 100-mL round bottom flask and stirred at 60 ºC for 5 days. The reaction was cooled to RT, and the particles were isolated by a series of centrifugation, decanting, and resuspension (5×) with THF/MeOH (1:3). Volatile materials were removed under vacuum to yield 1-DA-3 Au (0.98 g) as a magenta powder.

Figures 2–4 illustrate the synthetic route utilized to ultimately form the DA-linked PEG-b-PS copolymer ligand required for nanoparticle functionalization. Commercially available α-methoxy-ω-hydroxy PEG (Mn - 550 g/mol, PDI < 1.05) was treated with methane sulfonyl chloride to convert the ω-chain end into a mesylate. After the addition of maleimide, N alkylation occurred under basic conditions to yield α-methoxy-ω-maleimido PEG (polymer 1) in 95% yield (figure 2). Reversible addition fragmentation transfer (RAFT) polymerization of styrene was chosen to address the need for an α-furyl-ω-mercapto PS, as previous work has demonstrated the facile transformation of the dithioester chain end to a mercapto functionality (*25*, *30*). Furyl alcohol was transformed into a RAFT polymerization initiator in two steps with an overall yield of 85% (figure 3). Typical RAFT polymerization conditions of styrene utilize thermal initiation, in which radical formation occurs after a DA reaction between two styrene molecules. Attempts to use thermal initiation resulted in the preparation of PS, but an unwanted

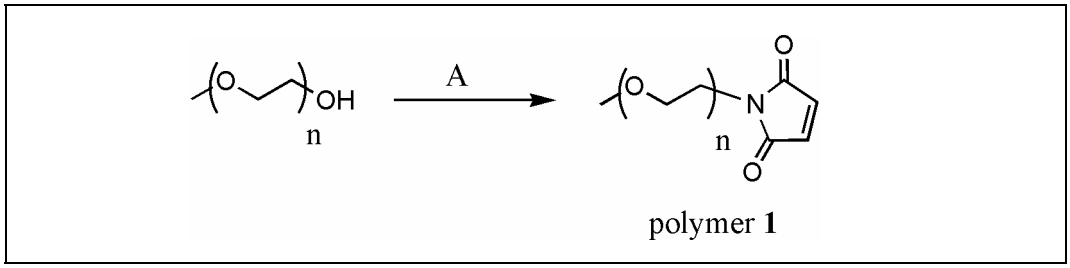

polymer **1**

Figure 2. Synthetic route for preparation of α-maleimido-ω-methoxy poly(ethylene glycol) (polymer 1). Conditions: (a) Et3N, MsCl, CH_2Cl_2, 0 ºC - RT, 4 hr; (b) solid K_2CO_3, maleimide, THF, reflux, 12 hr.

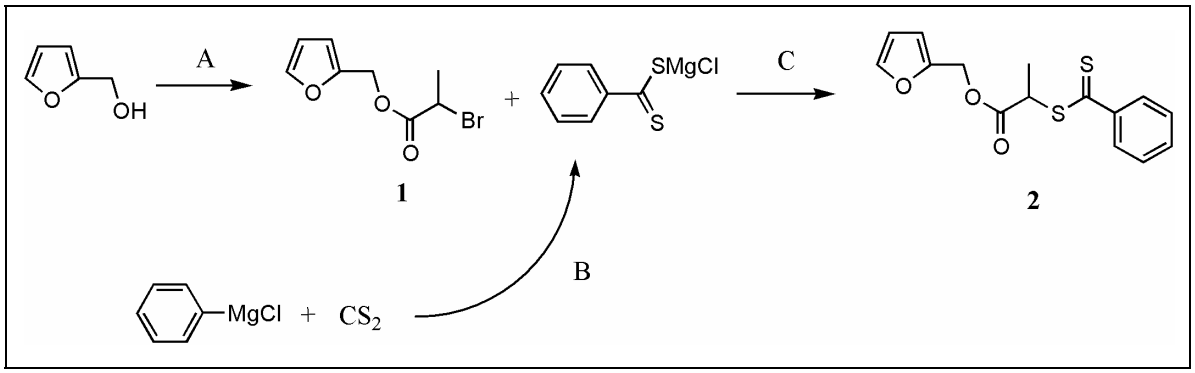

Figure 3. Synthetic route for preparation of RAFT initiator. Conditions: (a) Et3N, 2-bromopropionyl bromide, CH_2Cl_2, 0 ºC - RT, 12 hr; (b) THF, –78 ºC for 15 min, RT for 1 hr; (c) THF, RT, 5 hr.

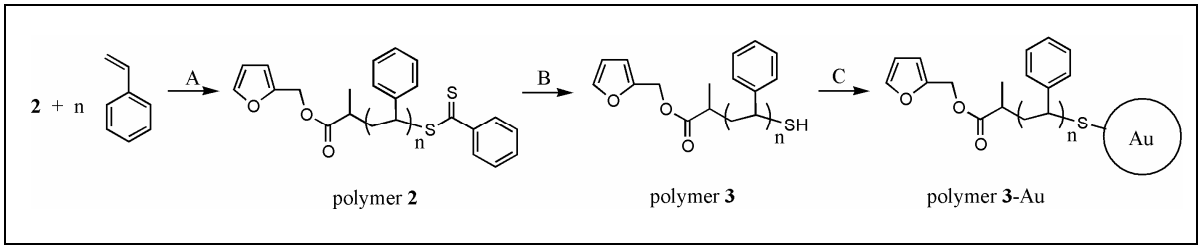

Figure 4. Synthetic route for preparation of furyl functionalized Au nanoparticles (polymer 3-Au). Conditions: (a) AIBN, THF, 70 ºC, 19 hr; (b) $NaBH_4$, EtOH, THF, RT, 20 hr; (c) toluene, reflux, 2 hr.

DA reaction occurred between a styrene molecule and the RAFT initiator, which eliminated the desired chain end functionality. Therefore, AIBN was employed as a radical source to reduce reaction temperatures and eliminate unwanted DA reactions, as shown in figure 4. Figure 5 displays a gel permeation chromatograph of polymer 2, illustrating a narrow Gaussian distribution typical of polymers prepared using RAFT polymerization.

Preliminary experiments demonstrated the ability to tether polymer 1 and polymer 2 via Diels-Alder reactions. α-Methoxy-ω-maleimido PEG was stirred at 60 ºC in THF with α-furyl-ω-S-thiobenzoyl PS for several days. After 5 days, the sample was precipitated in CH_3OH, and the isolated polymer was analyzed by ^1H NMR, shown in figure 1. The appearance of methylene peaks at 3.60 ppm confirmed the presence of polymer 2 demonstrating the ability to tether polymer 1 and polymer 2 together via a Diels-Alder reaction to yield the 1-DA-2 copolymer that is analogous to the polymer ligand needed for the compatibilization of the nanoparticles with the PEG matrix. To demonstrate the reversibility of this chemistry, the isolated 1-DA-2 copolymer was dissolved in toluene and heated at 90 ºC for 12 hr. The reaction mixture was precipitated into CH_3OH, and the resulting polymer was analyzed by ^1H NMR. The absence of methylene peaks at 3.60 ppm in figure 1 implied the Diels-Alder linkage had been severed. Polymer 2 precipitated upon addition of CH_3OH while polymer 1 remained in solution. Although not displayed, peaks at 1–3 ppm and 6.8–7.4 ppm typical of PS were also observed.

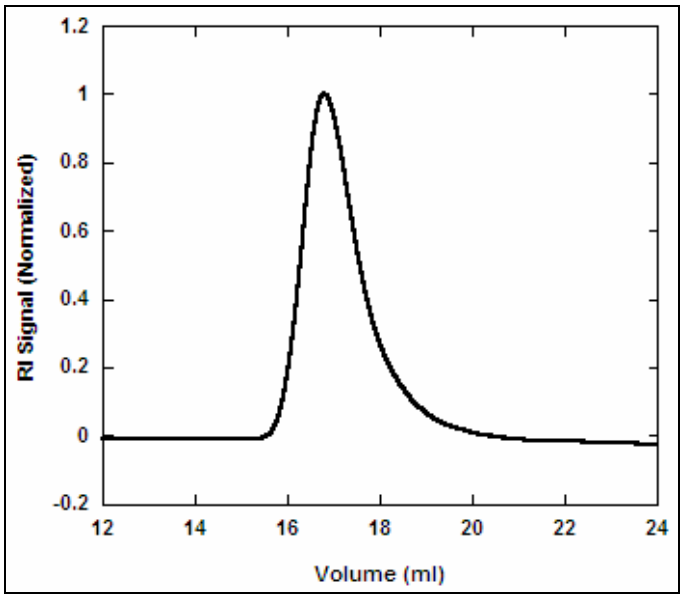

Figure 5. Gel permeation chromatograph of polymer 2.
M_n - 4,600; PDI - 1.14.

Au nanoparticles were prepared according to a previously published method (*31*), then characterized by SAXS and TEM. The SAXS data, fit using a log-normal size distribution for a spherical particle shape, are shown in figure 6. Also given in figure 6 are the volume distribution of particle sizes, the scattering data generated from the particle form factor, and the normalized residual. The particle size distribution mode was found to be 8.93 nm, the median 9.82 nm, and the mean 10.07 nm. Oscillations in the residual are most likely due to a small amount of interparticle scattering despite the low concentration, and the noise in the residual at large q is clearly due to a low signal-to-noise ratio.

Figure 7 depicts a typical TEM micrograph of oleylamine functionalized Au nanoparticles. Analysis using the ImageJ program, which is available free of charge from the NIH website (*26*), resulted in a nanoparticle diameter of 12 nm ± 7 nm, which is in good agreement with size distribution determined from SAXS. Minor deviations can be attributed to threshold and minimum pixel size utilized within the ImageJ analysis. In addition, the presence of multilayers of particles will skew analysis.

Next, α-furyl-ω-S-thiobenzoyl PS was treated with $NaBH_4$ to prepare α-furyl-ω-mercapto PS, polymer 3, which was utilized in a ligand exchange reaction to functionalize Au nanoparticles, polymer 3-Au, as shown in figure 4. Then, furyl functionalized Au nanoparticles were stirred at 60 ºC in THF with excess equivalents polymer 1 for several days to yield 1-DA-3 di-block copolymer functionalized Au nanoparticles, 1-DA-3 Au. Repeated cycles of centrifugation, decanting, and resuspension were used to remove excess polymer 1. The resulting 1-DA-3 Au was stored as a stock solution in THF. Figure 7 depicts a typical TEM micrograph of 1-DA-3 Au. The increased spacing between the nanoparticles indicates the presence of polymer and alludes to successful functionalization of the particles.

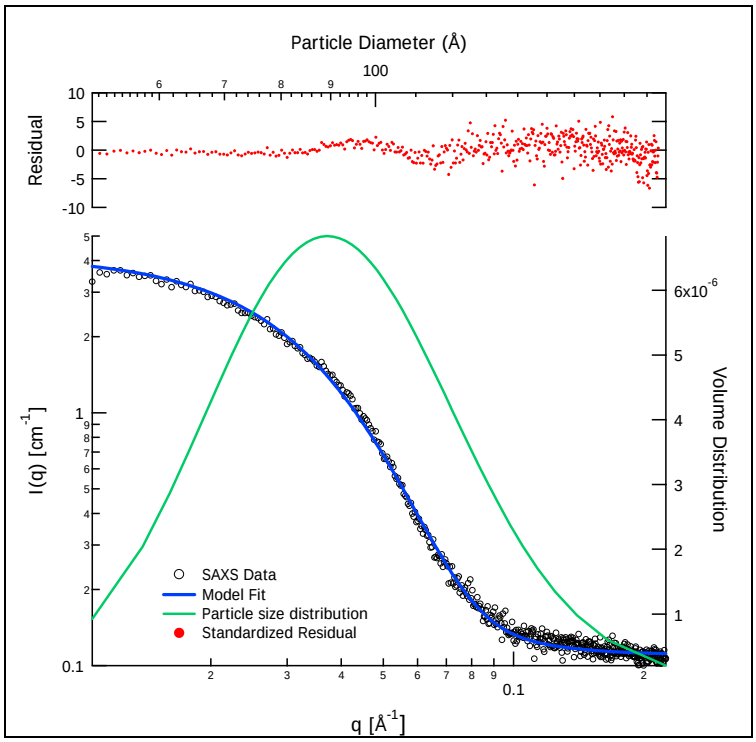

Figure 6. Analysis of SAXS data of Au nanoparticles yielding a particle size distribution of 8.9 nm ± 3 nm.

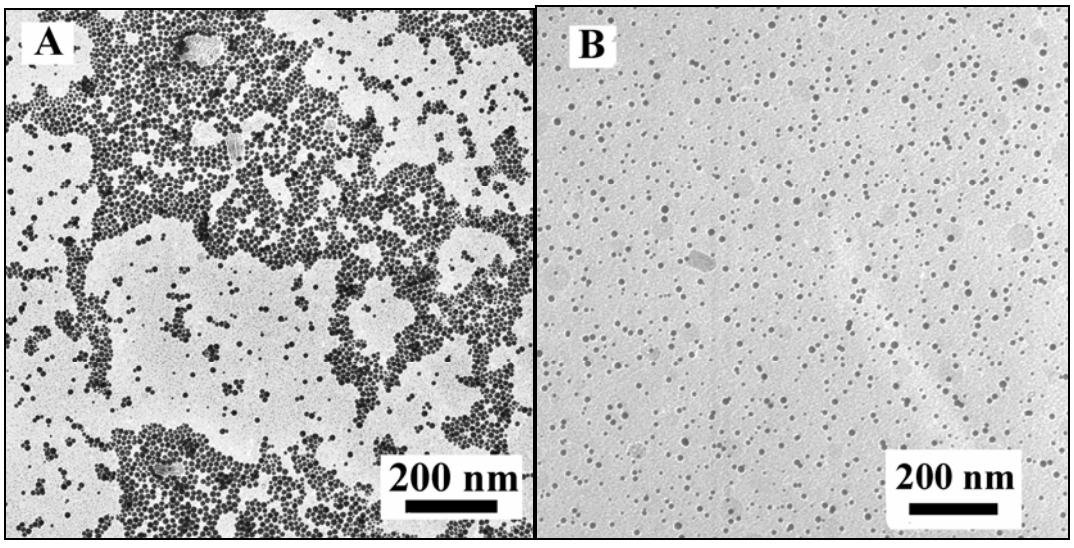

Figure 7. TEM analysis of (a) oleylamine functionalized Au nanoparticles (12 nm ± 7 nm) and (b) polymer 3-Au nanoparticles (11 nm ± 6 nm) displaying an increased spacing due to the presence of polymer 3.

Polymer films were then prepared by dissolving a PEG matrix (M_n - 2k or 5k; PDI < 1.05) in THF and adding various amounts of the 1-DA-3 Au stock solution. Slow evaporation of solvent reduced drying defects and resulted in polymer films with thicknesses ranging from 350–700 μm. The films were annealed at various temperatures and times and subsequently characterized by contact angle measurements, SAXS, and RBS to explore the migration of the functionalized Au particles within the PEG matrix.

3. Results and Discussion

Films were annealed at various temperatures and times and subsequently characterized by contact angle measurements, RBS, and SAXS to explore the location and migration of the functionalized Au particles within the poly(ethylene glycol) (PEG) matrix. RBS is a technique that allows the characterization of a surface to a depth of approximately 2 μm. A beam of ions, typically He^+, is targeted onto a surface. As the ions collide with the different atomic nuclei present in the film, some ions are absorbed while others backscatter. The scattering intensity is dependent upon the location and atomic mass of the nuclei.

Figure 8 depicts contact angle measurements of films composed of 2000-g/mol PEG containing 0.5 to 4 weight-percent of 1-DA-3 Au additive that were annealed at 60 ºC and 90 ºC for 24 hr. Anneal temperatures were chosen to shift the DA equilibrium towards the adduct (60 ºC) or individual components (90 ºC) illustrated in figure 9. After annealing at 60 ºC for 24 hr, the

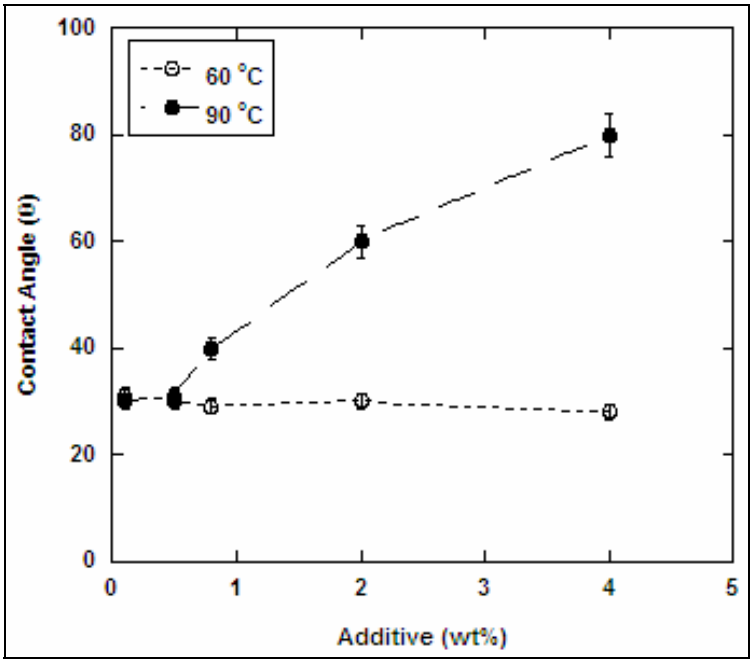

Figure 8. Contact angle measurement data for films comprised of 2k PEG containing various weight-percent of 1-DA-3 Au additive after annealing at 60 ºC and 90 ºC for 24 hr.

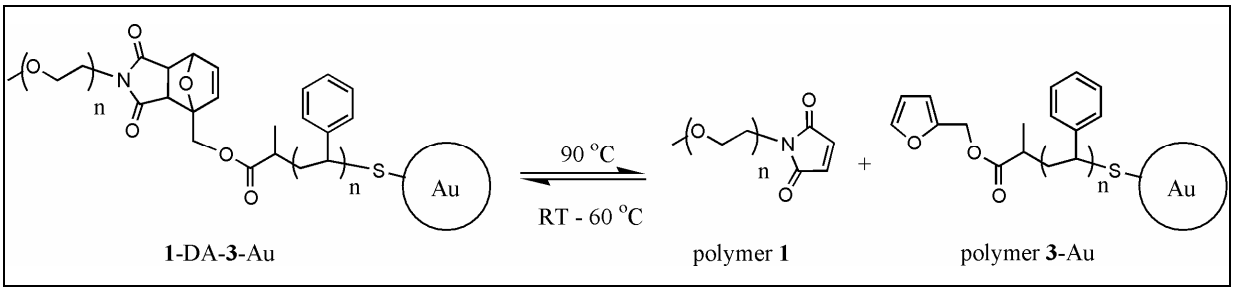

Figure 9. Proposed model system based upon Diels-Alder chemistry.

resulting contact angle was independent of the weight-percent of additive within the matrix and was within experimental error of pure PEG (30º ± 5º) (*32*). Thus, the PEG shell effectively served to compatiblize the PS-Au core from the surrounding PEG matrix.

RBS analysis of the same samples indicated that a small amount of particle migration occurred after annealing at 60 ºC (figure 10). At this temperature, the formation of the DA adduct is favored, but exists in equilibrium with the back reaction. Therefore, once the DA adduct is severed, polymer 1 is able to diffuse away into the PEG matrix; however, the high viscosity that exists at 60 ºC retards particle migration, which reduces the likelihood of reformation of the DA adduct, allowing minor phase separation. Allowing film formation to occur at RT resulted in a random distribution of Au particles.

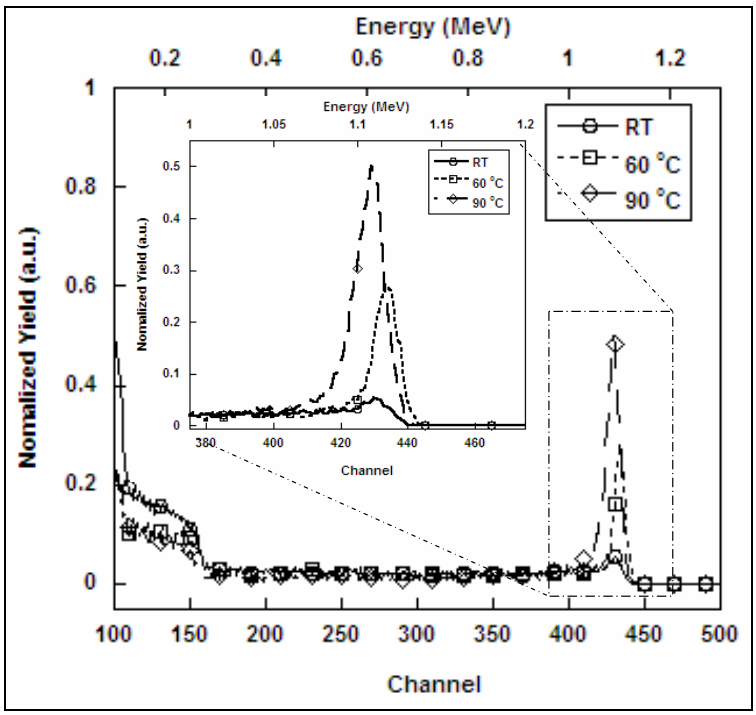

Figure 10. RBS analysis for films comprised of 2k PEG containing 4 weight-percent of 1-DA-3 Au additive after annealing at RT, 60 ºC and 90 ºC for 24 hr.

After annealing the films at 90 ºC for 24 hr, significant changes in the contact angle occur that are dependent upon the weight-percent of additive present. At 90 ºC, cleavage of the DA adduct is favored, and the decreased viscosity allows particle migration to occur. Such an increase in the contact angle indicates a reduction of surface energy that is most likely caused by the presence of the PS functionalized Au nanoparticles at the surface. RBS analysis displays a dramatic enhancement in the concentration of Au atoms at the surface and supports the notion of particle migration.

SAXS analysis of the films support these claims with the appearance of a Bragg-like peak after annealing at 60 ºC, shown in figure 11. As previously mentioned, the equilibrium nature of the DA reaction causes minor phase separation to reduce interaction energies between the exposed PS and the PEG matrix resulting in particle aggregation. After the films are annealed at 90 ºC, SAXS analysis indicates scattering from only the individual Au nanoparticles. In addition, the peak shape indicates that there is no higher ordering present, corresponding to a large aggregation of functionalized Au nanoparticles at the surface.

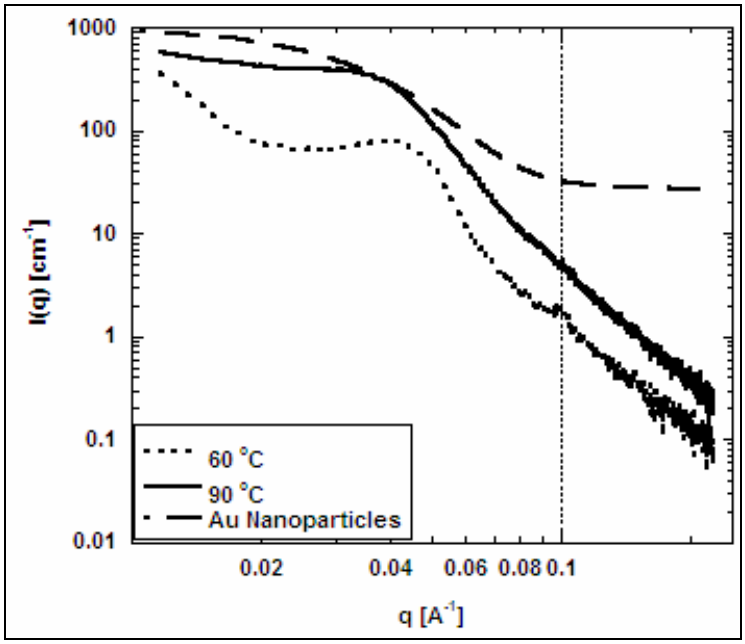

Figure 11. SAXS analysis for films comprised of 2k PEG containing 4 weight-percent of 1-DA-3 Au additive after annealing at 60 ºC and 90 ºC for 24 hr.

Control experiments were conducted to exemplify the need of each component of the proposed system. First, 5 weight-percent of polymer 3 was dispersed within a 5000-g/mol PEG matrix. Contact angle measurements of the corresponding films after annealing at 60 ºC and 90 ºC resulted in identical results of 58º ± 2º, indicating that for both annealing temperatures, the PS

preferentially phase separates to the air interface to reduce surface energy, resulting in a larger contact angle measurement than that of pure PEG.

Next, Au nanoparticles were functionalized with two different mercapto terminated polymers, α-mercapto-ω-methoxy PEG (Mn - 5k; PDI < 1.05) and a α-mercapto-ω-methoxy PS-b-PEG (Mn - 40k; PDI - 1.22; 88 weight-percent St), respectively. The functionalized Au nanoparticles were dispersed at 5 weight-percent in a 5000-g/mol PEG matrix and annealed at 60 ºC and 90 ºC for 24 hr. Contact angle measurements in conjunction with RBS analysis indicate that no particle migration occurred regardless of anneal temperature. These control experiments indicate three principles: (1) PS will phase separate to the air interface when dispersed within a PEG matrix to reduce surface energy, (2) PS is needed to induce migration of the Au particles, and (3) a DA linkage between the blocks is necessary to expose the PS-Au core to the PEG matrix.

In summary, poly(styrene) and poly(ethylene glycol) polymers with maleimide and furyl chain end functionality were prepared in high yield, then assembled using Diels-Alder reactions. Subsequently, Au nanoparticles were synthesized, functionalized with Diels-Alder assembled PS-b-PEG copolymers, and homogenously dispersed within a PEG matrix. Thermal treatment of the films was found to cleave the diblock copolymer, rendering the PS functionalized Au nanoparticles immiscible with the PEG matrices. This caused migration of the functionalized Au nanoparticles to the film surfaces as indicated by contact angle measurements, RBS analysis, and control experiments. Further investigations into the migration process are currently being explored.

4. References

1. Xu, F. J.; Zhong, S. P.; Yung, L. Y. L.; Neoh, K. G. Surface-Active and Stimuli-Responsive Polymer-S(100) Hybrids From Surface-Initiated Atom Transfer Radical Polymerization for Control of Cell Adhesion. *Biomacromolecules* **2004**, *5*, 2392–2403.

2. Okajima, S.; Sakai, Y.; Yamaguchi, T. Development of a Regenerable Cell Culture System That Senses and Releases Dead Cells. *Langmuir* **2005**, *21*, 4043–4049.

3. Csetneki, I.; Filipcsei, G.; Zrinyi, M. Smart Nanocomposite Polymer Membranes With On/Off Switching Control. Macromolecules, to be published.

4. Mcelhanon, H. R.; Russick, E. M.; Wheeler, D. R.; Low, D. A.; Aubert, J. H. Removable Foams Based on an Epoxy Resin Incorporating Reversible Diels-Alder Adducts. *J. Appl. Poly. Sci.* **2002**, *85*, 1496–1502.

5. Elman, J. F.; Johs, B. D.; Long, T. E.; Koberstein, J. T. A Neutron Reflectivity Investigation of Surface and Interface Segregations of Polymer Functional End Groups. *Macromolecules* **1994**, *27*, 5341.

6. Bhatia, Q. S.; Pan, D. H.; Koberstein, J. T. Perferential Surface Adsorption in Miscible Blends of Polystyrene and Poly(vinyl methyl ether). *Macromolecules* **1988**, *21*, 2166–2175.

7. Pan, D. H.; Prest, W. M. J. Surfaces of Polymer Blends-X-Ray Photoelectron-Spectroscopy Studies of Polystyrene/Poly(vinyl methyl-ether) Blends. *J. Appl. Phys.* **1985**, *58*, 2861.

8. Schmitt, R.; Gardella, J. A.; Magill, J. H.; Salvat, L. Study of Surface Composition and Morphology of Block Copolymers of Bisphenol A Polycarbonate and Poly(dimethylsiloxane) by X-ray Photoelectron Spectroscopy and Ion Scattering Spectroscopy. *Macromolecules* **1985**, *18*, 2675–2679.

9. Wu, S. *Polymer Interfaces and Adhesion*; 1st ed., Marcel Dekker: New York, NY, 1982.

10. Gaines, G. L. Surface Tension of Polymer Solutions. I Solutions of Poly(dimethylsiloxanes). *J. Chem. Phys.* **1969**, *73*, 3143.

11. Hunt, M. O. J.; Belu, A. M.; Linton, R. W.; DeSimone, J. M. Poly(ether esters) From Pivalolactone, Alkanediols, and Dimethyl Terephthalate. 1. Synthesis, Structure Analysis, and Reaction Mechanism. *Macromolecules* **1993**, *26*, 4845–4853.

.

12. Affrossman, S.; Hartshorne, M.; Kiff, T.; Pethrick, R. A.; Richards, R. W. Surface Segregation in Blends of Hydrogenous Polystyrene and Perfluorohexane End-Capped Deuterated Polystrene, Studied by SSIMS and XPS. *Macromolecules* **1994**, *27*, 1588–1591.

13. Hopkinson, I.; Kiff, F. T.; Richards, R. W.; Bucknall, D. G.; Clough, A. S. Equilibrium Concentration Profiles of Physically End Tethered Polystyrene Molecules at the Air-Polymer Interface. *Polymer* **1997**, *38*, 87.

14. Schaub, T. F.; Kellogg, G. J.; Mayes, A. M.; Kulasekere, R.; Anker, J. F.; Kaiser, H. Surface Modification Via Chain End Segregation in Polymer Blends. *Macromolecules* **1996**, *29*, 3982–3990.

15. Mason, R.; Jalbert, C. J.; O'Rourke-Muisener, P. A. V.; Koberstein, J. T. Adaptive and Responsive Surfaces Through Controlled Reorganization of the Interfacial Polymer Layers. *Adv. Colloid Interface Sci.* **2001**, *94*, 1.

16. Yuan, C.; Ouyang, M.; Koberstein, J. T. Effects of Low-Energy End Groups on the Dewetting Dynamics of Poly(styrene) Films on Poly(methyl metharcrylate) Substrates. *Macromolecules* **1999**, *32*, 2329–2333.

17. Jalbert, C. A.; Koberstein, J. T.; Hariharan, A.; Kumar, S. End Group Effects on Surface Properties of Polymers: Semiempirical Calculations and Comparison to Experimental Surface Tensions for a,w-Functional Poly(dimethylsiloxanes). *Macromolecules* **1997**, *30*, 4481–4490.

18. O'Rourke-Muisener, P. A. V.; Koberstein, J. T.; Kumar, S. Optimal Chain Architectures for the Molecular Design of Functional Polymer Surfaces. *Macromolecules* **2003**, *36*, 771-781.

19. O'Rourke-Muisener, P. A. V.; Jalber, C. A.; Yuan, C.; Baetzold, J.; Mason, R.; Wong, D.; Kim, Y. J.; Koberstein, J. T. Measurement and Modeling of End Group Concentration Depth Profiles for w-Fluorosilane Polystyrene and Its Blends. *Macromolecules* **2003**, *36*, 2956–2966.

20. Fringuelli, F.; Taticchi, A. *Dienes in the Diels-Alder Reaction*; John Wiley & Sons: New York, NY, 1990.

21. Carruthers, W. *Cycloaddition Reactions in Organic Synthesis*; Elsevier Publishing Company: Oxford, U.K., 1990.

22. Imai, Y.; Itoh, H.; Naka, K.; Chujo, Y. Thermally Reversible IPN Organic-Inorganic Polymer Hybrids Utilizing the Diels-Alder Reaction. *Macromolecules* **2000**, *33*, 4343–4346.

23. Gheneim, R.; Perez-Berumen, C.; Gandini, A. Diels-Alder Reactions With Novel Polymeric Dienes and Dienophiles: Synthesis of Reversible Cross-Linked Elastomers. *Macromolecules* **2002**, *35*, 7246–7253.

24. Chen, X.; Wudl, F.; Mal., A. K.; Shen, H. B.; Nutt, S. R. New Thermally Remendable Highly Cross-Linked Polymeric Materials. *Macromolecules* **2003**, *36*, 1802–1807.

25. Costanzo, P. J. In *Chemistry*; University of California, Davis: Davis, CA, 2005.

26. National Institute of Health. http://rsb.info.nih.gov/ij/download.html (accessed 2006).

27. Doolittle, L. R. A Semiautomatic Algorithm for Rutherford Backscattering Analysis. *Nuclear Instruments and Methods* **1986**, *B15*, 227.

28. Russell, T. P.; Lin, J. S.; Spooner, S.; Wignall, G. D. Intercalibration of Small-Angle X-Ray and Neutron Scattering Data. *J. Applied Crystallography* **1988**, *21*, 628–538.

29. Feigin, L. A.; Svergun, D. I. *Structure Analysis by Small-Angle X-Ray and Neutron Scattering*; Springer: New York, NY, 1987.

30. Lowe, A. B.; Sumerlin, B. S.; Donovan, M. S.; McCormick, C. L. Facile Reparation of Transition Metal Nanoparticles Stabilized by Well-Defined (Co)Polymers Synthesized Via Aqueous Reversible Addition-Fragmentation Chain Transfer Polymerization. *J. Am. Chem. Soc.* **2002**, *124*, 11562–11563.

31. Hiramatsu, H.; Osterloh, F. E. A Simple Large-Scale Synthesis of Nearly Monodisperse Gold and Silver Nanoparticles With Adjustable Sizes and With Exchangeable Surfactants. *Chem. Mater.* **2004**, *16*, 2509–2511.

32. Prime, K. L.; Whitesides, G. M. Adsorption of Proteins Onto Surfaces Containing End-Attached Oligo(ethylene oxide): A Model System Using Self-Assembled Monolayers. *J. Am. Chem. Soc.* **1993**, *115*, 10714–10721.

NO. OF
COPIES ORGANIZATION

1 (PDF ONLY) DEFENSE TECHNICAL INFORMATION CTR
DTIC OCA
8725 JOHN J KINGMAN RD
STE 0944
FORT BELVOIR VA 22060-6218

1 US ARMY RSRCH DEV & ENGRG CMD
SYSTEMS OF SYSTEMS INTEGRATION
AMSRD SS T
6000 6TH ST STE 100
FORT BELVOIR VA 22060-5608

1 DIRECTOR
US ARMY RESEARCH LAB
IMNE ALC IMS
2800 POWDER MILL RD
ADELPHI MD 20783-1197

3 DIRECTOR
US ARMY RESEARCH LAB
AMSRD ARL CI OK TL
2800 POWDER MILL RD
ADELPHI MD 20783-1197

ABERDEEN PROVING GROUND

1 DIR USARL
AMSRD ARL CI OK TP (BLDG 4600)

INTENTIONALLY LEFT BLANK.